Dalton Transactions

ROYAL SOCIETY OF CHEMISTRY

PAPER

View Article Online
View Journal | View Issue

Cite this: *Dalton Trans.*, 2022, **51**, 4903

$Na_4Ga_8S_{14}$: a Ga-enriched wide band gap ternary alkali-metal sulfide with unique $[Ga_{12}S_{42}]$ 12-membered rings†

Ling Luo,‡[a,b] Linan Wang,‡[c] Chen Bai,[d] Jiazheng Zhou,*[a,b] Lai Wei[a,b] and Xin Su *[a,b]

A Ga-enriched ternary alkali-metal sulfide $Na_4Ga_8S_{14}$ has been synthesized by a high temperature solid-state reaction. It crystallizes in the centrosymmetric *Pbca* (no. 61) space group with cell parameters a = 13.5260(4) Å, b = 11.4979(3) Å, c = 29.9592(9) Å, and Z = 8, and exhibits a three-dimensional (3D) network structure constructed from unique $[Ga_{12}S_{42}]$ 12-membered rings, one-dimensional $_\infty[Ga_4S_{11}]$ chains, individual $[GaS_4]$ units and Na^+ ions. The experimental band gap of $Na_4Ga_8S_{14}$ was measured as ~3.57 eV. Theoretical calculations indicate that the title compound is a direct band gap compound and the band gap is mainly determined by $[GaS_4]$ units. Meanwhile, statistical analysis shows that the atomic ratio N (N = A^IA^{II}/Ga, where A^I = alkali-metal, A^{II} = alkaline earth-metal) can be used to regulate the connection of $[GaS_4]$ units from zero-dimensional (0D) isolated groups, one-dimensional (1D) chains, and two-dimensional (2D) layers to 3D frameworks in Ga-containing alkali- and/or alkaline earth-metal chalcogenides. The results enrich the diversity of alkali-metal sulfides and give an insight into the structural regulation of alkali- and/or alkaline earth-metal chalcogenides.

Received 30th January 2022,
Accepted 22nd February 2022

DOI: 10.1039/d2dt00295g

rsc.li/dalton

1. Introduction

The development of structural chemistry and the exploration of new functional materials depend on the discovery of new compounds with distinctive crystal structures.[1–9] Metal chalcogenides have recently attracted great interest in photoelectric functional materials,[10–14] especially in infrared (IR) nonlinear optical (NLO) materials, due to their abundant structural diversity and adjustable band gaps.[15–17] To enlarge the band gap and enhance the laser-induced damage threshold (LIDT) of chalcogenides, introduction of alkali- and/or alkaline earth-metals has been demonstrated as a feasible method.[18–21]

Recently, a great number of alkali- and/or alkaline earth-metal chalcogenides with wide band gaps have been developed by high temperature solid-state reactions.[22,23] For example, in 2008 Ye *et al.* reported the fabrication of IR NLO material $BaGa_4S_7$,[24] which exhibited a large band gap, high LIDT, wide optically transparent region, and suitable second-order susceptibility coefficients. After that, in 2010, Wu, Yao and co-workers reported the fabrication of α-$BaGa_4Se_7$ with enhanced NLO coefficients compared with $BaGa_4S_7$.[25] To regulate the band gap of quaternary metal chalcogenides, alkali metal and alkaline-earth metal LiS_4 and MgS_4 tetrahedral units were simultaneously introduced into the quaternary chalcogenides, and, most recently, the first alkali and alkaline-earth diamond-like IR NLO material $Li_4MgGe_2S_7$ with an exceptionally large band gap (4.12 eV) and a high LIDT (7 × $AgGaS_2$ at 1064 nm) was successfully developed by Pan and co-workers.[26]

In this work, taking $BaGa_4S_7$ as the reference, we investigated the Na–Ga–S system and reported a Ga-enriched alkali-metal ternary sulfide $Na_4Ga_8S_{14}$. The compound crystallizes in the orthorhombic *Pbca* space group (no. 61) with cell parameters a = 13.5260(4) Å, b = 11.4979(3) Å, c = 29.9592(9) Å, and Z = 8. Different from the formed 6-membered ring-like tunnel structure in $BaGa_4S_7$, $Na_4Ga_8S_{14}$ shows a complex 3D network structure constructed by rare $[Ga_{12}S_{42}]$ 12-membered rings, one-dimensional $_\infty[Ga_4S_{11}]$ chains, individual $[GaS_4]$ units and Na^+ ions. Statistical analyses on the structures of Ga-contain-

[a]*School of Physical Science and Technology, Yili Normal University, Yining 835000, China. E-mail: suxin_phy@sina.com, phy_zhoujiazheng@sina.com*
[b]*Xinjiang Laboratory of Phase Transitions and Microstructures of Condensed Matter Physics, Yi Li Normal University, Yining 835000, China*
[c]*Center of Materials Science and Optoelectronics Engineering, University of Chinese Academy of Sciences, Beijing 100049, China*
[d]*College of Chemistry and Chemical Engineering, Xinjiang Normal University, Urumqi, Xinjiang 830054, China*

†Electronic supplementary information (ESI) available: Experimental details, related figures, tables and crystal data. CCDC 2145472 for $Na_4Ga_8S_{14}$. For ESI and crystallographic data in CIF or other electronic format see DOI: 10.1039/d2dt00295g

‡These authors contributed equally.

ing alkali- and/or alkaline earth-metal chalcogenides indicate that the atomic ratio N (N = A^IA^{II}/Ga, where A^I = alkali-metal, A^{II} = alkaline earth-metal) plays a critical role in determining the dimensions of [GaS_4] units in the compounds. With the decrease of the atomic ratio N, the [GaS_4] units show a structure transformation from zero-dimensional (0D) isolated groups, one-dimensional (1D) chains, and two-dimensional (2D) layers to 3D frameworks. The experimental optical band gap of $Na_4Ga_8S_{14}$ is ~3.57 eV, close to that of 3.54 eV in $BaGa_4S_7$.[24] Theoretical calculations show that $Na_4Ga_8S_{14}$ is a direct band gap compound, and the band gap is mainly determined by the [GaS_4] tetrahedron. Moreover, the birefringence of $Na_4Ga_8S_{14}$ was calculated to be 0.004@1064 nm.

2. Experimental sections

2.1 Chemical syntheses

Na, Ga, and S elemental substances with a high purity of 99.9% were used for the syntheses of $Na_4Ga_8S_{14}$ single crystal and pure phase powder samples. All starting chemicals were obtained from Aladdin Industrial Corporation and used without further purification.

$Na_4Ga_8S_{14}$ single crystals were prepared by high temperature solid state reactions *via* the following procedure: (1) Na, Ga and S powders in a molar ratio of 2 : 4 : 7 were weighed and loaded into quartz tubes with an inner diameter of 10 mm; (2) the tubes were then flame-sealed in a vacuum of ~10^{-3} Pa; (3) the sealed tubes were placed into a computer-controlled muffle furnace, heated to 900 °C in 70 h, and kept at this temperature for 70 h; the temperature was then decreased slowly to room temperature at a cooling rate of 6 °C h^{-1}. Finally, the plate-like colorless crystals were harvested. The $Na_4Ga_8S_{14}$ pure phase powder samples were prepared by following a similar synthesis process, with the reaction temperature set to 850 °C.

2.2 Crystal structure determination

A Bruker D8 Venture using Mo Kα radiation (λ = 0.71073 Å) was used for the determination of the single crystal structure at room temperature. After collection, the SADABS program was used to perform the multiscan-type absorption correction of the structural data.[27] Afterwards the XPREP program in the SHELXTL program package was used to determine the space group, and the SHELXT and XL programs were used to solve and refine the structural data by direct methods and full-matrix least-squares on F^2.[28] Finally the PLATON program was used to check the possible missing symmetry elements, and no higher symmetry was found.[29,30] The crystal data and structure refinement, atomic coordinates and bond-valence sum (BVS), selected bond lengths and angles, and equivalent isotropic displacement parameters are listed in Tables S1–S5.†

2.3 Energy-dispersive X-ray spectroscopy (EDS)

The EDS spectrum of the title compound was characterized on a field emission scanning electron microscope (FE-SEM, JEOL JSM-7610F Plus, Japan) equipped with an energy-dispersive X-ray spectrometer (Oxford, X-Max 50), which was operated at 5 kV.

2.4 Powder X-ray diffraction (PXRD)

A Bruker D2 PHASER diffractometer with Cu Kα radiation (λ = 1.5418 Å) was used to record the PXRD diffraction patterns and to check the purity of powder samples. The collected angular 2θ range was set to 10–70° with a scan rate of 0.02°.[31] The theoretical XRD pattern was calculated by Mercury software based on the $Na_4Ga_8S_{14}$ CIF file. The powder XRD Rietveld refinement was implemented using GSAS software.[32–35]

2.5 UV-Vis-NIR diffuse reflectance spectroscopy

A Shimadzu SolidSpec-3700DUV spectrophotometer was used to record the diffuse reflectance spectrum of the title compound at room temperature.[36,37] Then, the Kubelka–Munk function, $F(R) = \alpha/S = (1 - R)^2/2R$ (where $F(R)$ is the ratio of absorption coefficient to scattering coefficient; α is the absorption coefficient; R the reflectance; S the scattering coefficient) was used to calculate the absorption spectrum from the reflection spectrum and the bandgap was determined.[38–42]

2.6 Theoretical calculations

The first-principles calculations were performed by the plane wave pseudopotential method implemented with the CASTEP package.[43] The Generalized Gradient Approximation (GGA) and Perdew–Burke–Ernzerhof (PBE) functional were employed in the calculations,[44] and the norm-conserving pseudopotentials (NCP) were used to calculate electronic structure and optical properties.[45] The energy cut-off was set to 800.0 eV for the title compound. To simulate the effective interactions between valence electrons and the atomic cores, the valence electrons were set as $3s^1$ for Na, $4s^2\ 4p^1$ for Ga and $3s^2\ 3p^4$ for S and the Monkhorst–Pack k-point grids were set as 3 × 3 × 1 in the Brillouin Zone (BZ).

Besides, the Heyd–Scuseria–Ernzerhof 06 (HSE06) hybrid functional[46–48] was employed using the PWmat code runs on graphics processing unit processors (GPU). The NCPP-SG15-PBE pseudo-potential and 50 Ryd plane wave cut-off energy were used in the calculation:

$$E_{XC}^{HSE} = \alpha E_X^{HF,SR}(\mu) + (1-\alpha)E_X^{PBE,SR}(\mu) + E_X^{PBE,LR}(\mu) + E_C^{PBE} \quad (1)$$

(α: mixing parameter; μ: adjustable parameter controlling the short-range of the interaction; $E_X^{HF,SR}(\mu)$: short range Hartree–Fock exact exchange functional; $E_X^{PBE,SR}(\mu)$ and $E_X^{PBE,LR}(\mu)$: short and long range components of the PBE exchange functional; E_C^{PBE}: PBE correlation functional). In HSE06, the parameters are suggested as α = 0.25.

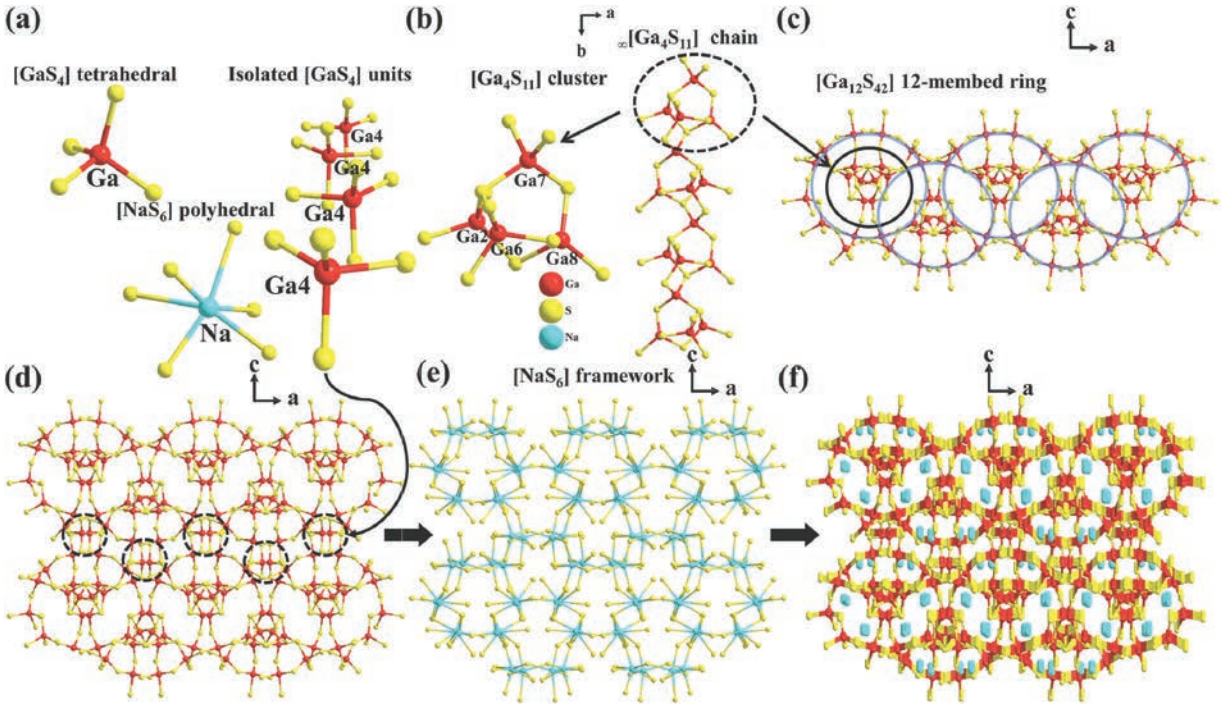

Fig. 1 (a) The coordination environments of Na and Ga atoms; (b) the $[Ga_4S_{11}]$ cluster and the formed $_\infty[Ga_4S_{11}]$ one-dimensional infinite chain; (c) the $[Ga_{12}S_{42}]$ 12-membered ring; (d) the formed Ga–S 3D framework structure along the *b* direction; (e) the formed $[NaS_6]$ 3D framework structure along the *b* direction; (f) the whole 3D structure of $Na_4Ga_8S_{14}$ viewed along the *b* direction.

3. Results and discussion

3.1 Crystal structure

$Na_4Ga_8S_{14}$ crystallizes in the centrosymmetric *Pbca* space group (no. 61) with cell parameters a = 13.5260(4) Å, b = 11.4979(3) Å, c = 29.9592(9) Å, and Z = 8. In the asymmetric unit of the title compound, there are four crystallographically independent Na atoms, eight Ga atoms and fourteen S atoms, which are located at Wyckoff 8*c* positions. Meanwhile, the BVS analyses indicate that all the atoms are in reasonable oxidation states (Table S2†). The Ga atoms are coordinated with four S atoms to form $[GaS_4]$ tetrahedral units with Ga–S bond lengths of 2.220–2.408 Å (Fig. 1a and S1, Table S3†).[49] The Na atoms are connected with six S atoms to build $[NaS_6]$ polyhedral groups with Na–S bond lengths of 2.740–3.531 Å (Fig. 1a and S1, Table S3†).[50] The $[Ga2S_4]$, $[Ga6S_4]$, $[Ga7S_4]$ and $[Ga8S_4]$ units are connected with each other to build $[Ga_4S_{11}]$ clusters by sharing corners, which are further connected to construct a $_\infty[Ga_4S_{11}]$ one-dimensional infinite chain along the *b* axis by sharing S atoms (Fig. 1b). The $[Ga1S_4]$, $[Ga3S_4]$, $[Ga5S_4]$, $[Ga6S_4]$ and $[Ga8S_4]$ units are organized to form $[Ga_{12}S_{42}]$ 12-membered ring-like tunnels (marked by blue rings in Fig. 1c), and the $_\infty[Ga_4S_{11}]$ chains (marked by a black ring in Fig. 1c) are located in the center of the tunnels. The formed ring-like tunnels are nested with each other, and are further connected *via* the individual $[GaS_4]$ units (marked by the black rings in Fig. 1d) to construct the Ga–S 3D framework (Fig. 1d). The Na^+ ions are located in the tunnels to balance the charge and result in the final 3D structures of the title compound (Fig. 1e and f).

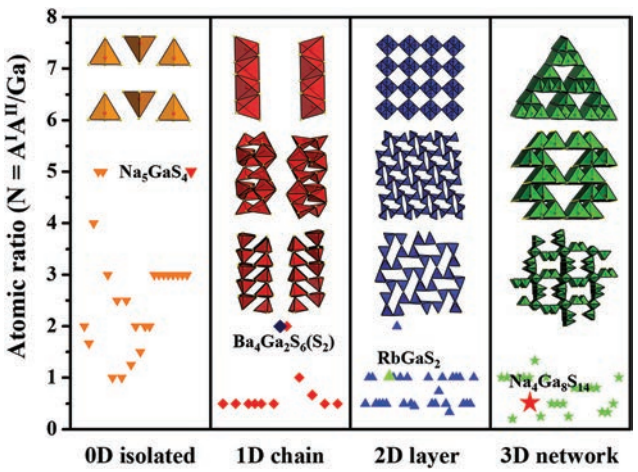

Fig. 2 The relationship between the A^IA^{II}/Ga (A^I = alkali-metal, A^{II} = alkaline earth-metal) atomic ratio and the dimensions of GaQ_4 (Q = S, Se) tetrahedral units in Ga-containing alkali/alkaline earth metal chalcogenides.

To investigate the influence of alkali- and/or alkaline earth-metals on crystal structures in chalcogenides, a statistical analysis was conducted. By searching the Ga-containing alkali metal and/or alkaline earth metal chalcogenides in the Inorganic Crystal Structure Database (ICSD), 88 target compounds were found for the structure comparisons. The statistical results (Fig. 2) indicate

that the atomic ratio N (N = A^IA^{II}/Ga, where A^I = alkali–metal, A^{II} = alkaline earth-metal) plays a critical role in determining the dimensions of [GaS_4] units in the compounds. Specifically, with the increase of Ga atoms, the [GaS_4] units show a structure transformation from 0D isolated groups, 1D chains, and 2D layers to 3D frameworks. For example, from Na_5GaS_4 (N = 5),[51] to $Ba_4Ga_2S_6(S_2)$ (N = 2),[52] $MGaS_2$ (M = Na and Rb; N = 1),[53,54] and $BaGa_4S_7$ (N = 0.25),[24] the linked GaS_4 units show a transformation from isolated 0D [GaS_4] clusters, to 1D $[Ga_2S_7]_n$ chains, 2D $[GaS_2]_n$ layers and 3D $[GaS_3]_n$ networks. Interestingly, for the tunnel-like Ga–S 3D frameworks, the shape of the tunnels shows abundant diversity. Different from the 6-membered ring tunnel-like 3D framework in $BaGa_4S_7$, $BaGa_4Se_7$ and $LiGaS_2$,[20,24,25,55] and the 12-membered ring rectangular tunnel-like 3D framework in $LiBa_4Ga_5Se_{12}$,[49] the formed 12-membered ring-like tunnels in $Na_4Ga_8S_{14}$ are rarely reported.

3.2 Optical properties

To evaluate the experimental band gap of the title compound, the pure phase powder samples were synthesized and characterized by a high temperature solid-state reaction. The powder XRD Rietveld refinement was carried out. The refined R_p and R_{wp} values are 4.63% and 6.31%, respectively, confirming the phase purity of the synthesized $Na_4Ga_8S_{14}$ polycrystalline powder samples. Furthermore, the PXRD patterns of $Na_4Ga_8S_{14}$ powder samples before and after exposure to air or to water indicate that $Na_4Ga_8S_{14}$ is comparably stable (Fig. S2†).

To check the chemical composition and bonding in $Na_4Ga_8S_{14}$, EDS and Raman spectra of the crystalline samples were investigated. The EDS spectrum demonstrates the existence of Na, Ga and S elements in the sample with a quantified atomic ratio of Na : Ga : S = 4.0 : 7.3 : 15.1 (Table S6,† Fig. 3b and S3†), matched with the stoichiometric ratio in the formula of $Na_4Ga_8S_{14}$. The Raman spectrum confirms the existence of Na–S and Ga–S bonding. As shown in Fig. 3c, the peaks below 200 cm^{-1} can be attributed to the characteristic vibrations of Na–S bonding, while the peaks around 336, 374 and 394 cm^{-1} can be attributed to the characteristic vibrations of the Ga–S bond in the GaS_4 tetrahedral units.[49,56–58]

The UV-vis-NIR diffuse reflectance spectrum of the title compound was measured using the synthesized pure phase polycrystalline powder samples. To evaluate the experimental band gap of the title compound, the UV-vis-NIR diffuse reflectance spectrum was transformed to the absorption spectrum based on the Kubelka–Munk function. The experimental band gap (E_g) of $Na_4Ga_8S_{14}$ is measured as ~3.57 eV (Fig. 3d), which is comparable to the value in Ga-enriched $BaGa_4S_7$ (3.54 eV),[24] and is larger than the values in $PbGa_4S_7$ (3.08 eV)[59] and $SnGa_4S_7$ (3.1 eV).[60] The results indicate that the introduction of alkali metal/alkaline earth-metal is beneficial for enlarging the band gap of ternary chalcogenide compounds, which is similar to the cases in the quaternary chalcogenides, such as in Cu_2ZnGeS_4 (2.2 eV)[61] and α-Li_2ZnGeS_4 (4.07 eV),[62] as well as in Li_4HgGeS_7 (2.75 eV)[63] and $Li_4MgGe_2S_7$ (4.12 eV).[26]

3.3 Theoretical calculations

To clarify the origin of the optical band and to evaluate the birefringence of the title compound, the first-principles calculations based on density functional theory (DFT) were carried out. The calculated band gap structure with GGA indicates that $Na_4Ga_8S_{14}$ is a direct band gap compound since both the valence band (VB) maximum and the conduction band (CB) minimum are located at the G point as shown in Fig. 4a, and the calculated band gap is 2.699 eV. Furthermore, based on the calculated PDOS as shown in Fig. 4b, the bottom of the CB is mainly occupied by Ga 4*s* and the VB maximum is mainly occupied by S 3*p* states. To further confirm the contribution of Ga atoms (there are 8 crystallographically independent Ga atoms in the structure) to the band gap, each Ga PDOS was further analyzed in detail. As shown in Fig. 4c, Ga1 4*s* states make a significant contribution to the bottom of the CB in contrast to other Ga atoms. Hence, based on the results in Fig. 4b and c, it can be concluded that the band gap of the

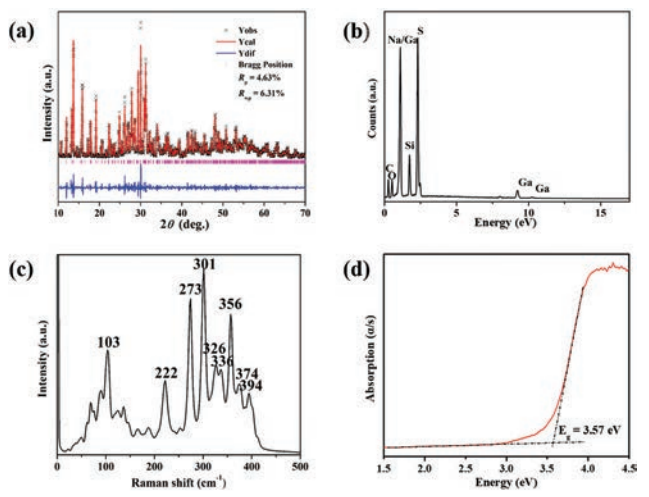

Fig. 3 (a) The Rietveld refinement PXRD patterns of $Na_4Ga_8S_{14}$; (b) EDS spectrum; (c) Raman spectrum; and (d) the experimental band gap of $Na_4Ga_8S_{14}$.

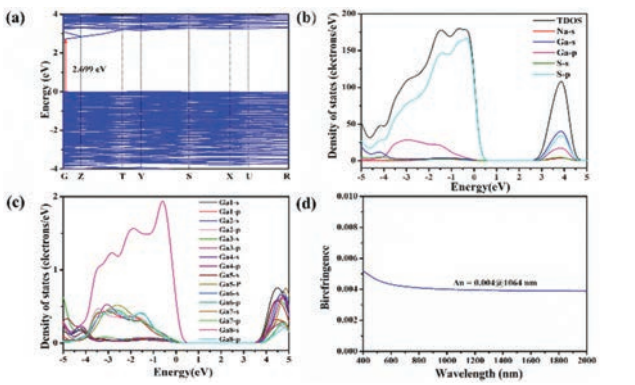

Fig. 4 The calculated band structures (a), density of states (DOS) (b), partial DOS (c), and calculated birefringence (d) of $Na_4Ga_8S_{14}$.

title compound is mainly determined by Ga–S bonding in [$Ga1S_4$] units. It's worth noting that, the band gap calculated by GGA is much smaller than the experimental result (3.57 eV) because of the discontinuity of the exchange–correlation energy functional. To ensure the accuracy of the calculated band gap of the title compound, the HSE06 functional was also employed.[64–66] The calculated HSE06 band gap of $Na_4Ga_8S_{14}$ is ~3.58 eV, which is in good agreement with the experimental result (3.57 eV). In addition, the birefringence of $Na_4Ga_8S_{14}$ is calculated to be ~0.004@1064 nm (Fig. 4d).

4. Conclusions

In summary, a Ga-enriched ternary alkali-metal sulfide $Na_4Ga_8S_{14}$ has been synthesized by a high temperature solid-state reaction. The compound exhibits a complex 3D tunnel structure with rare [$Ga_{12}S_{42}$] 12-membered rings. The statistical analysis confirms that the crystal structure and the connection of [GaS_4] units in Ga-containing alkali- and/or alkaline earth-metal chalcogenides can be effectively regulated by adjusting the atomic ratio of alkali- and/or alkaline earth-metal to Ga atoms in the compounds. The experimental optical band gap of the title compound is measured as ~3.57 eV, which is comparable to the value in Ga-riched $BaGa_4S_7$ (3.53 eV) and is larger than those in $PbGa_4S_7$ (3.08 eV) and $SnGa_4S_7$ (3.1 eV). Meanwhile, the calculated results show that the title compound is a direct band gap compound, and the band gap is mainly determined by the Ga–S bonding in [$Ga1S_4$] units.

Conflicts of interest

The authors declare no conflict of interest.

Acknowledgements

This work was completed under the help of Natural Science Foundation of Xinjiang Uygur Autonomous Region of China (Grant No. 2018D01C005 and 2018Q077), the "13th Five-Year" Key Disciplines of Xinjiang Uygur Autonomous Region (Grant No. XJZDXK-phy201810), and the National Natural Science Foundation of China (Grant No. 11847072).

Notes and references

1 H. P. Wu, B. B. Zhang, H. W. Yu, Z. G. Hu, J. Y. Wang, Y. C. Wu and P. S. Halasyamani, *Angew. Chem., Int. Ed.*, 2020, **59**, 8922–8926.
2 C. Bai, B. L. Cheng, K. W. Zhang, M. Zhang, S. L. Pan and J. J. Li, *Dalton Trans.*, 2021, **50**, 16401–16405.
3 M. Mutailipu, M. Zhang, B. B. Zhang, L. Y. Wang, Z. H. Yang, X. Zhou and S. L. Pan, *Angew. Chem., Int. Ed.*, 2018, **57**, 6095–6099.
4 M. Mutailipu, K. R. Poeppelmeier and S. L. Pan, *Chem. Rev.*, 2021, **121**, 1130–1202.
5 Z. X. Fan, C. Bai, H. S. Shi, M. Zhang, B. Zhang, J. Zhang and J. J. Li, *Dalton Trans.*, 2021, **50**, 14038–14043.
6 J. J. Li, Y. P. Li, Q. Li, Z. C. Wang and F. L. Deepak, *Nanoscale Horiz.*, 2019, **4**, 1302–1309.
7 J. Y. Guo, A. Tudi, S. J. Han, Z. H. Yang and S. L. Pan, *Angew. Chem., Int. Ed.*, 2021, **60**, 24901–24904.
8 J. J. Li, J. C. Chen, H. Wang, N. Chen, Z. C. Wang, L. Guo and F. L. Deepak, *Adv. Sci.*, 2018, **5**, 1700992.
9 Q. Wu, C. Yang, X. Liu, J. Ma, F. Liang and Y. S. Du, *Mater. Today Phys.*, 2021, **21**, 100569.
10 J. Z. Zhou, Y. Chu, J. J. Li and S. L. Pan, *Chem. Commun.*, 2021, **57**, 6440–6443.
11 K. Wu, B. B. Zhang, Z. H. Yang and S. L. Pan, *J. Am. Chem. Soc.*, 2017, **139**, 14885–14888.
12 Y. Huang, L. Gao, H. H. Yu, Z. H. Yang, J. J. Li and S. L. Pan, *Chem. – Eur. J*, 2021, **27**, 6538–6544.
13 G. M. Li, J. J. Li, K. Wu, Z. H. Yang and S. L. Pan, *Chem. Commun.*, 2019, **55**, 14793–14796.
14 H. B. Gao, R. J. Chen, K. W. Zhang, A. Abudurusuli, K. R. Lai and J. J. Li, *Dalton Trans.*, 2021, **50**, 6315–6320.
15 Y. Chu, P. Wang, H. Zeng, S. C. Cheng, X. Su, Z. H. Yang, J. J. Li and S. L. Pan, *Chem. Mater.*, 2021, **33**, 6514–6521.
16 A. Abudurusuli, J. J. Li and S. L. Pan, *Dalton Trans.*, 2021, **50**, 3155–3160.
17 G. M. Li, Z. H. Yang, J. J. Li and S. L. Pan, *Chem. Commun.*, 2020, **56**, 11565–11576.
18 D. J. Mei, W. Z. Cao, N. Z. Wang, X. X. Jiang, J. Zhao, W. K. Wang, J. H. Dang, S. Y. Zhang, Y. D. Wu, P. H. Rao and Z. S. Lin, *Mater. Horiz.*, 2021, **8**, 2330–2334.
19 Y. Yang, Y. Chu, B. B. Zhang, K. Wu and S. L. Pan, *Chem. Mater.*, 2021, **33**, 4225–4230.
20 Z. Qian, Q. Bian, H. P. Wu, H. W. Yu, Z. S. Lin, Z. G. Hu, J. Y. Wang and Y. C. Wu, *J. Mater. Chem. C*, 2021, **10**, 96–101.
21 Y. Chu, G. M. Li, X. Su, K. Wu and S. L. Pan, *J. Solid State Chem.*, 2019, **271**, 266–272.
22 H. Li, G. M. Li, K. Wu, B. B. Zhang, Z. H. Yang and S. L. Pan, *Chem. Mater.*, 2018, **30**, 7428–7432.
23 Y. Chu, K. Wu, X. Su, J. Han, Z. H. Yang and S. L. Pan, *Inorg. Chem.*, 2018, **57**, 11310–11313.
24 X. S. Lin, G. Zhang and N. Ye, *Cryst. Growth Des.*, 2009, **9**, 1186–1189.
25 J. Y. Yao, D. J. Mei, L. Bai, Z. S. Lin, W. L. Yin, P. Z. Fu and Y. C. Wu, *Inorg. Chem.*, 2010, **49**, 9212–9216.
26 A. Abudurusuli, J. B. Huang, P. Wang, Z. H. Yang, S. L. Pan and J. J. Li, *Angew. Chem., Int. Ed.*, 2021, **60**, 24131–24136.
27 L. Haeming and G. M. Sheldrick, *Acta Crystallogr., Sect. A: Found. Crystallogr.*, 1999, **55**, 206–206.
28 G. M. Sheldrick, *Acta Crystallogr., Sect. A: Found. Crystallogr.*, 2008, **64**, 112–122.
29 A. L. Spek, *J. Appl. Crystallogr.*, 2003, **36**, 7–13.
30 X. F. Wang, Y. Wang, B. B. Zhang, F. F. Zhang, Z. H. Yang and S. L. Pan, *Angew. Chem., Int. Ed.*, 2017, **56**, 14119–14123.

31 X. L. Chen, B. B. Zhang, F. F. Zhang, Y. Wang, M. Zhang, Z. H. Yang, K. R. Poeppelmeier and S. L. Pan, *J. Am. Chem. Soc.*, 2018, **140**, 16311–16319.
32 J. Z. Zhou, L. Luo, Y. Chu, P. Wang, Z. Y. Guo, X. Su and J. J. Li, *J. Alloys Compd.*, 2022, **899**, 163366.
33 B. H. Toby, *J. Appl. Crystallogr.*, 2001, **34**, 210–213.
34 C. C. Jin, X. P. Shi, H. Zeng, S. J. Han, Z. Chen, Z. H. Yang, M. Mutailipu and S. L. Pan, *Angew. Chem., Int. Ed.*, 2021, **60**, 20469–20475.
35 M. Xia, F. M. Li, M. Mutailipu, S. J. Han, Z. H. Yang and S. L. Pan, *Angew. Chem., Int. Ed.*, 2021, **60**, 14650–14656.
36 H. P. Wu, H. W. Yu, Z. H. Yang, X. L. Hou, X. Su, S. L. Pan, K. R. Poeppelmeier and J. M. Rondinelli, *J. Am. Chem. Soc.*, 2013, **135**, 4215–4218.
37 H. P. Wu, S. L. Pan, K. R. Poeppelmeier, H. Li, D. Jia, Z. Chen, X. Fan, Y. Yang, J. M. Rondinelli and H. Luo, *J. Am. Chem. Soc.*, 2011, **133**, 7786–7790.
38 J. Tauc, *Mater. Res. Bull.*, 1970, **5**, 721–729.
39 C. Bai, Y. Chu, J. Z. Zhou, L. A. Wang, L. Luo, S. L. Pan and J. J. Li, *Inorg. Chem. Front.*, 2022, **9**, 1023–1030.
40 C. Yang, X. Liu, C. L. Teng, X. H. Cheng, F. Liang and Q. Wu, *Mater. Today Phys.*, 2021, **19**, 100432–100439.
41 J. Y. Guo, A. Tudi, S. J. Han, Z. H. Yang and S. L. Pan, *Angew. Chem., Int. Ed.*, 2021, **60**, 3540–3544.
42 C. C. Jin, H. Zeng, F. Zhang, H. T. Qiu, Z. H. Yang, M. Mutailipu and S. L. Pan, *Chem. Mater.*, 2022, **34**, 440–450.
43 J. P. Perdew, K. Burke and M. Ernzerhof, *Phys. Rev. Lett.*, 1997, **78**, 1396–1396.
44 A. M. Rappe, K. M. Rabe, E. Kaxiras and J. D. Joannopoulos, *Phys. Rev. B: Condens. Matter Mater. Phys.*, 1990, **41**, 1227–1230.
45 D. Vanderbilt, *Phys. Rev. B: Condens. Matter Mater. Phys.*, 1990, **41**, 7892–7895.
46 J. Heyd, G. E. Scuseria and M. Ernzerhof, *J. Chem. Phys.*, 2003, **118**, 8207–8215.
47 A. V. Krukau, O. A. Vydrov, A. F. Izmaylov and G. E. Scuseria, *J. Chem. Phys.*, 2006, **125**, 224106.
48 C. M. Huang, M. Mutailipu, F. F. Zhang, K. J. Griffith, C. Hu, Z. H. Yang, J. M. Griffin, K. R. Poeppelmeier and S. L. Pan, *Nat. Commun.*, 2021, **12**, 2597–2597.
49 A. Abudurusuli, J. J. Li, T. H. Tong, Z. H. Yang and S. L. Pan, *Inorg. Chem.*, 2020, **59**, 5674–5682.
50 G. M. Li, K. Wu, Q. Liu, Z. H. Yang and S. L. Pan, *J. Am. Chem. Soc.*, 2016, **138**, 7422–7428.
51 S. Balijapelly, P. Sandineni, A. Adhikary, N. N. Gerasimchuk, A. V. Chernatynskiy and A. Choudhury, *Dalton Trans.*, 2021, **50**, 7372–7379.
52 J. W. Liu, P. Wang and L. Chen, *Inorg. Chem.*, 2011, **50**, 5706–5713.
53 Y. h. Yun, W. L. Xie, Z. H. Yang, G. M. Li and S. L. Pan, *J. Alloys Compd.*, 2022, **896**, 163093.
54 B. W. Liu, X. M. Jiang, H. Y. Zeng and G. C. Guo, *J. Am. Chem. Soc.*, 2020, **142**, 10641–10645.
55 A. Tyazhev, V. Vedenyapin, G. Marchev, L. Isaenko, D. Kolker, S. Lobanov, V. Petrov, A. Yelisseyev, M. Starikova and J. J. Zondy, *Opt. Mater.*, 2013, **35**, 1612–1615.
56 A. N. Yadav and K. Singh, *ACS Omega*, 2019, **4**, 18327–18333.
57 A. H. Reshak and S. Azam, *J. Magn. Magn. Mater.*, 2014, **362**, 204–215.
58 K. Wu, Z. H. Yang and S. L. Pan, *Chem. Mater.*, 2016, **28**, 2795–2801.
59 X. S. Li, L. Kang, C. Li, Z. S. Lin, J. Y. Yao and Y. C. Wu, *J. Mater. Chem. C*, 2015, **3**, 3060–3067.
60 W. D. Cheng, C. S. Lin, H. Zhang, Y. Z. Huang and G. L. Chai, *ChemPhysChem*, 2017, **18**, 519–525.
61 I. Tsuji, Y. Shimodaira, H. Kato, H. Kobayashi and A. Kudo, *Chem. Mater.*, 2010, **22**, 1402–1409.
62 J. H. Zhang, D. J. Clark, J. A. Brant, K. A. Rosmus, P. Grima, J. W. Lekse, J. I. Jang and J. A. Aitken, *Chem. Mater.*, 2020, **32**, 8947–8955.
63 K. Wu, Z. H. Yang and S. L. Pan, *Chem. Commun.*, 2017, **53**, 3010–3013.
64 B. B. Zhang, G. Q. Shi, Z. H. Yang, F. F. Zhang and S. L. Pan, *Angew. Chem., Int. Ed.*, 2017, **56**, 3916–3919.
65 G. Q. Shi, Y. Wang, F. F. Zhan, B. B. Zhang, Z. H. Yang, X. L. Hou, S. L. Pan and K. R. Poeppelmeier, *J. Am. Chem. Soc.*, 2017, **139**, 10645–10648.
66 Y. Wang, B. B. Zhang, Z. H. Yang and S. L. Pan, *Angew. Chem., Int. Ed.*, 2018, **57**, 2150–2154.